Supplemental Figure 1

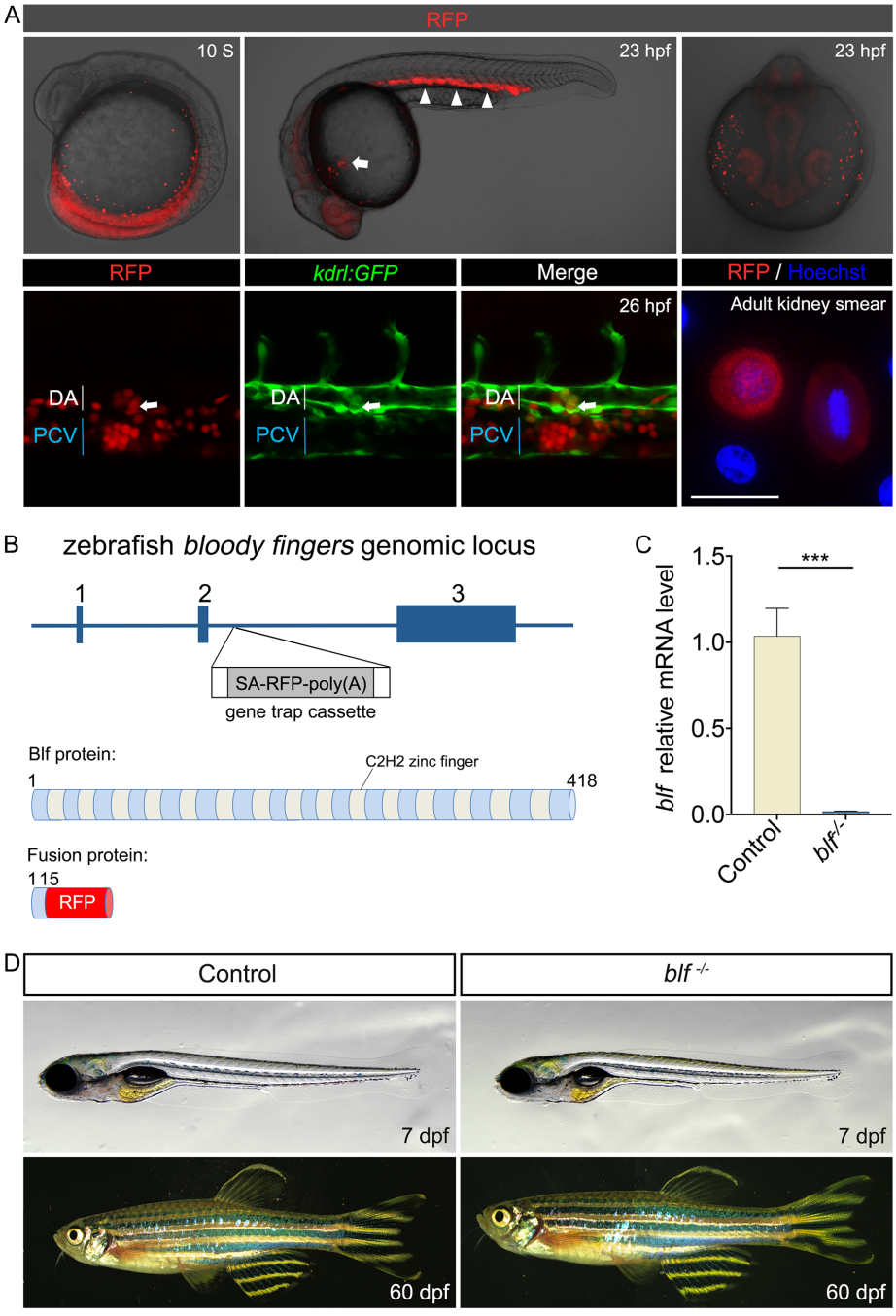

Fig. S1. Identification of the gene trapping line RP2-527. (**A**) RFP expression pattern in zebrafish gene trapping line RP2-527. At the 10 somite stage, RFP signal emerged in the bilateral stripes of the posterior lateral-plate mesoderm. Before circulation begins, RFP signal

could be observed in both the intermediate cell mass (white arrow) and the anterior hematopoietic site (white arrow). At 26 hpf, some RFP postive cells co-expressed the blood vessel endothelium reporter *flk1:GFP* and were indeed localized in the ventral side of dorsal aorta, demonstrating that these cells were hemogenic endothelial cells. In adult RP2-527 fish, an RFP signal could be observed in HSC-like cells in kidney. (**B**) Upper panel, the zebrafish *bfl* genomic locus. The transposon is inserted in the 2nd intron. Lower panel, schematic representations of the domain structure of the wild type zebrafish Blf protein and the fusion protein in RP2-527 fish. (**C**) QPCR results showing the absence of *blf* mRNA in RP2-527 homozygous embryos. Data are mean ± SEM of at least three replicates. ***P<0.001. (**D**) Live images of control (wild type) and *blf*$^{-/-}$ animals at the designated time points. Lateral view with head to left.

Supplemental Figure 2

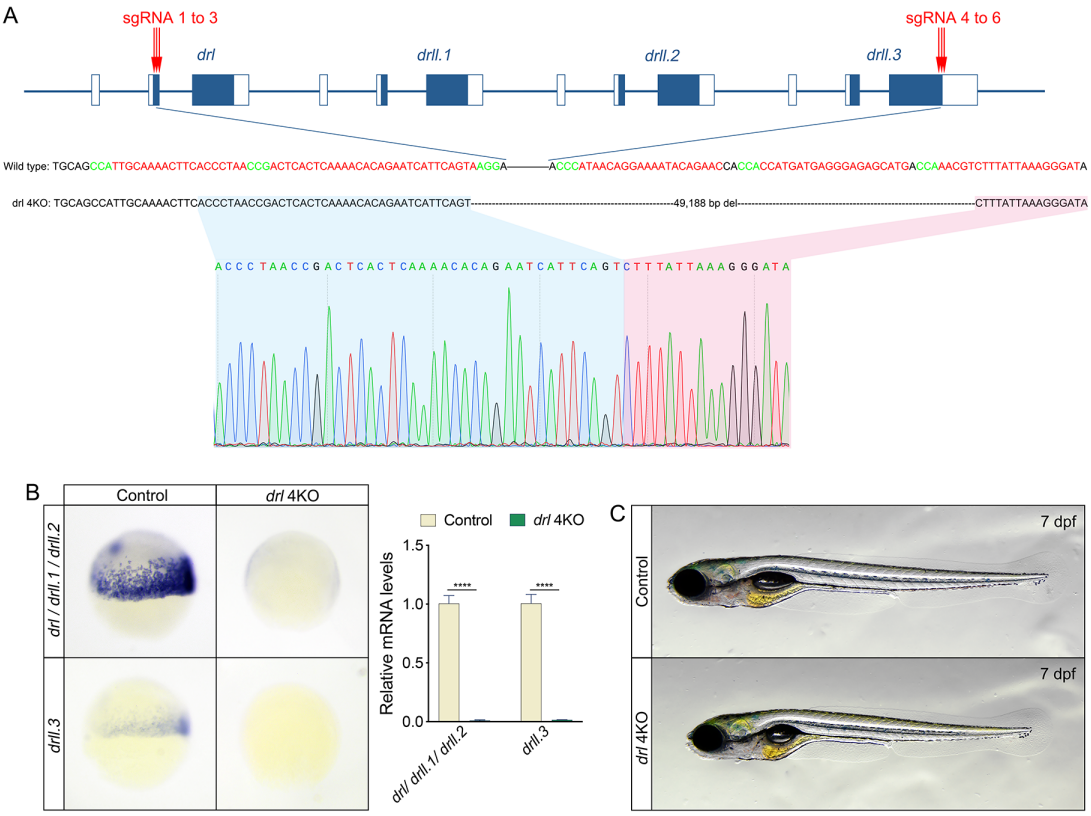

Fig. S2. Generation of *drl* cluster knockout zebrafish line. (**A**) Upper panel, the zebrafish *drl* cluster genomic locus and Cas9/sgRNA targeting sites. Lower panel, Sanger sequencing of genotyping PCR products indicating the 49,188 bp deletion on the *drl* cluster locus. (**B**) Whole mount *in situ* hybridization and qPCR results showing the absence of *drl* cluster genes mRNA in *drl* 4KO embryos. Data are mean ± SEM of at least three replicates. ****P<0.0001. (**C**) Live images of control (wild type) and *drl* 4KO fish at 7 days post fertilization. Lateral view with head to left.

Supplemental Figure 3

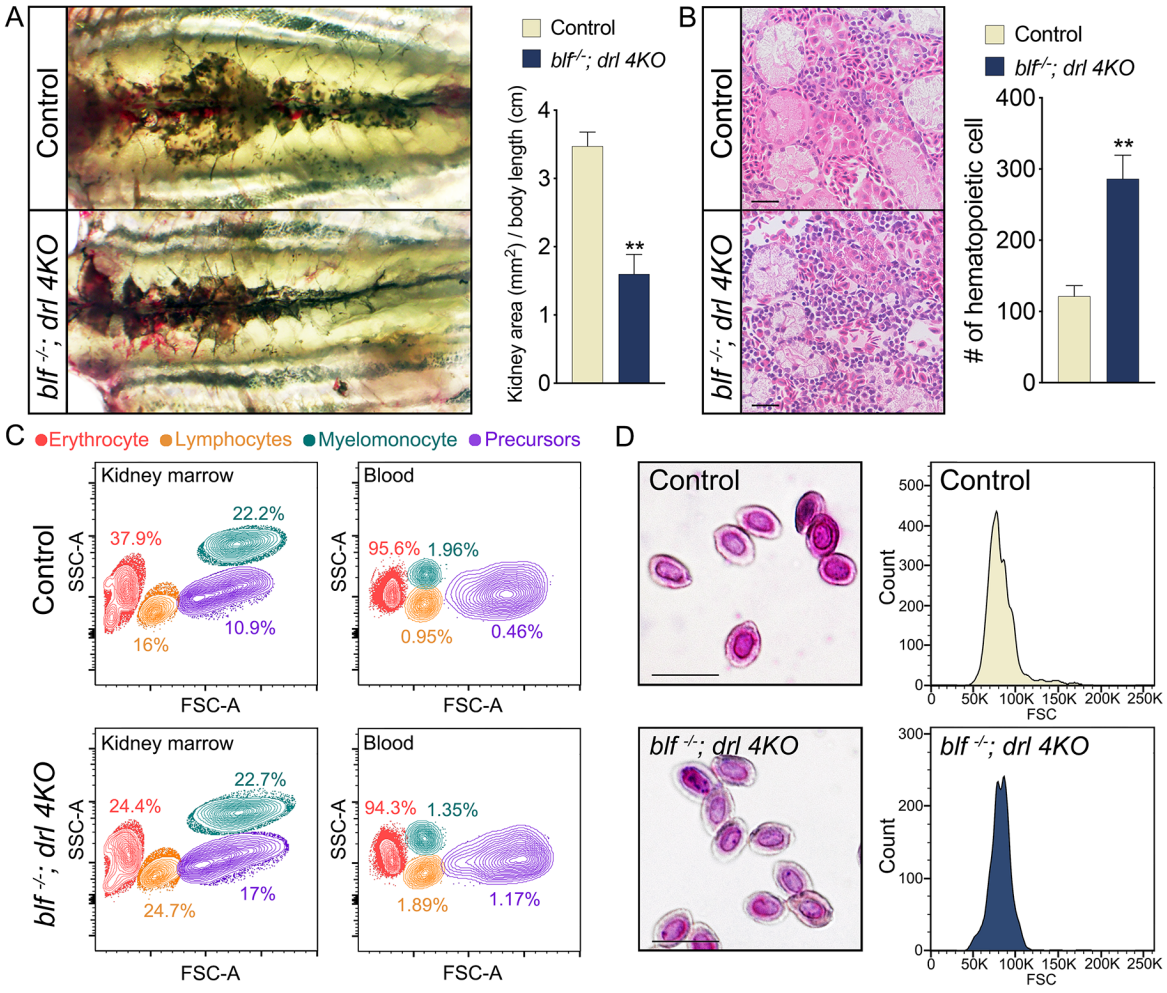

Fig. S3. Microscopic observation and hematological analysis of adult *blf*$^{-/-}$; *drl* 4KO fish. (**A**) Left panels, brightfield images of adult zebrafish kidney. The retroperitoneal hematopoietic kidney tissue appears as a dark flattened structure. Kidney size were measured and are reported relative to body length. (**B**) Photomicrographs of hematoxylin and eosin stained sections of head kidneys. Hematopoietic cells could be found between the renal tubules. Scale bar: 20 μm. Number of hematopoietic cells was counted on a 150μm x150μm field. (**C**) Representative flow cytometry plots from single cell suspensions from the dissected kidney and peripheral blood. Forward scatter (FSC) and side scatter (SSC) are proportional to cell size and cellular granularity, respectively. Four major populations were delineated: erythroid (red), lymphoid/erythroblast (brown), myeloid (green), and the immature precursor cells (purple). (**D**) Left panels, Wright-Giemsa staining of peripheral blood cells from adult zebrafish. Red blood cells are

terminally differentiated with elliptical morphology and condensed nuclei. Scale bar: 10 μm. Right panels, mean cell volume of red blood cells of adult control and *blf*$^{-/-}$; *drl* 4KO fish, cells from 2 genotypes have a similarly distributed volume. A, B, C and D at least 6 fish from each genotype were examined and representative results are shown. A and B, data are mean ± SEM, **P<0.01.

Supplemental Figure 4

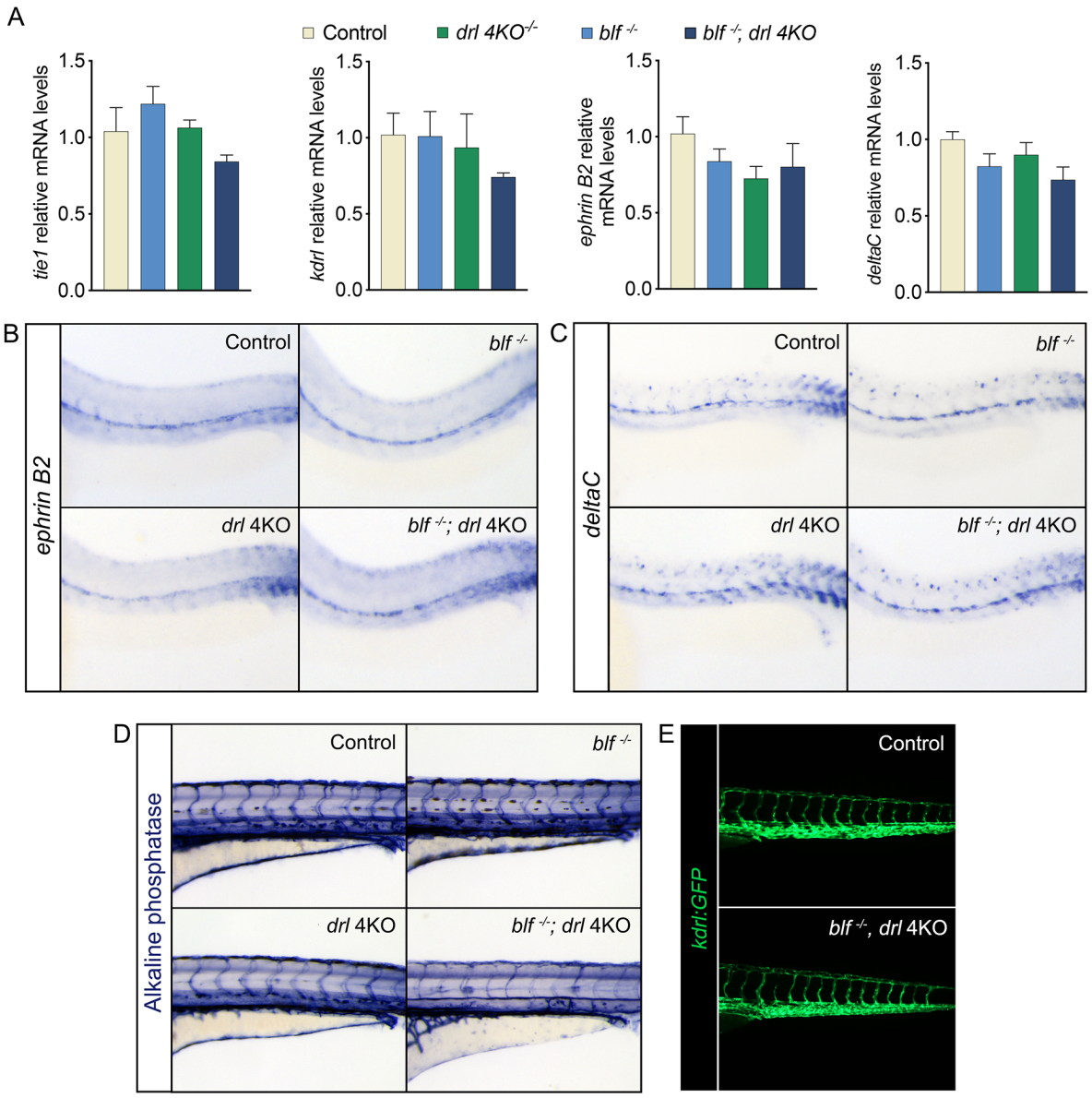

Fig. S4. *Blf* and *drl* cluster genes are dispensable for vasculature development. (**A**) QPCR results for the expression of *tie1*, *kdrl*, *ephrin B2* and *deltaC*. *Tie1* and *kdrl* are examined at 8 somite stage, *ephrin B2* and *deltaC* are examined at 24 hpf. Data are mean ± SEM of at least three replicates. (**B**) RNA *in situ* hybridization results for the expression of *ephirin B2* and *deltaC* in 24 hpf embryos. Lateral view with head to left. For *ephirin B2* WISH, n=38, 31, 39 and 33 for each genotype. For *deltaC* WISH, n=32, 37, 39 and 35 for each genotype. (**D**) Alkaline phosphatase

staining reveals the structure of intersegmental vessels at 72 hpf, n=32, 29, 28 and 30 for each genotype. (**E**) Fluorescence micrographs of wild type and *blf*$^{-/-}$; *drl* 4KO embryos in Tg(*kdrl:eGFP*) transgenic background 72 hpf. In comparation with wild type embryos, *blf*$^{-/-}$; *drl* 4KO embryo display similar patterns of intersegmental vessel and caudal vein. D and E, at least 8 embryos from each genotype were examined and representative results are shown.

Supplemental Figure 5

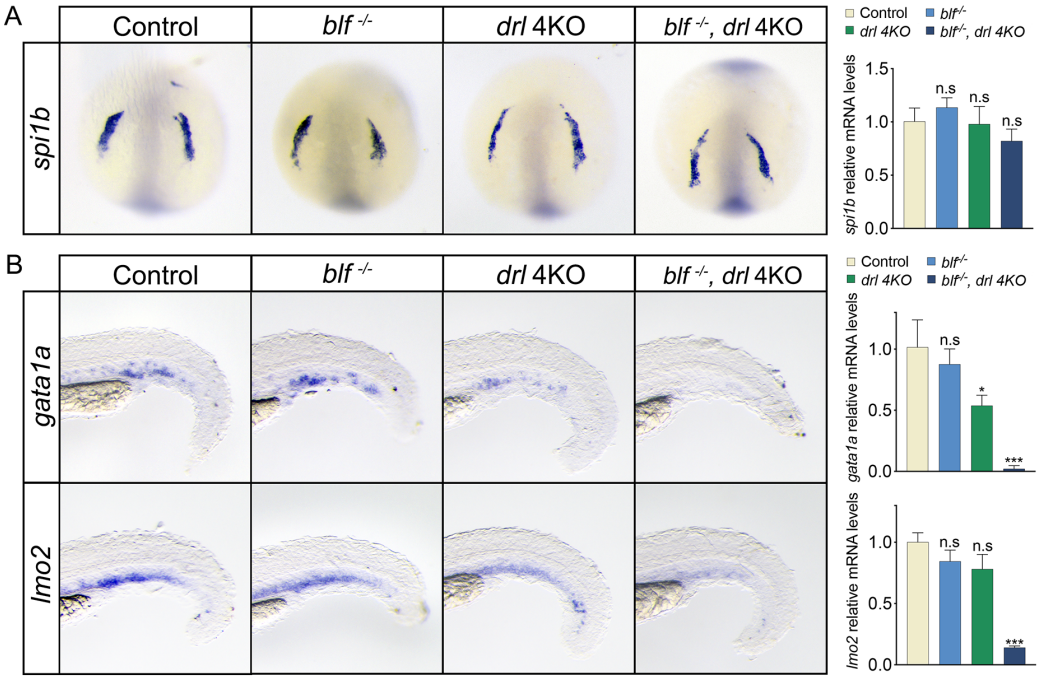

Fig. S5. The effect of loss of *blf* and *drl* cluster genes on primitive myelopoiesis and the formation of erythromyeloid progenitors. (**A**) RNA in situ hybridization and qPCR results for expression of *spi1b* in 8 somite embryos, n=26, 33, 31 and 40 for each genotype. Data are mean ± SEM of at least three replicates. n.s, not significant. (**B**) RNA in situ hybridization and qPCR results for expression of *gata1a* (n=39, 35, 31 and 27) and *lmo2* (n=34, 30, 26 and 32) in 30 hpf embryos. Data are mean ± SEM of at least three replicates. n.s, not significant, ***P<0.001.

Supplemental Figure 6

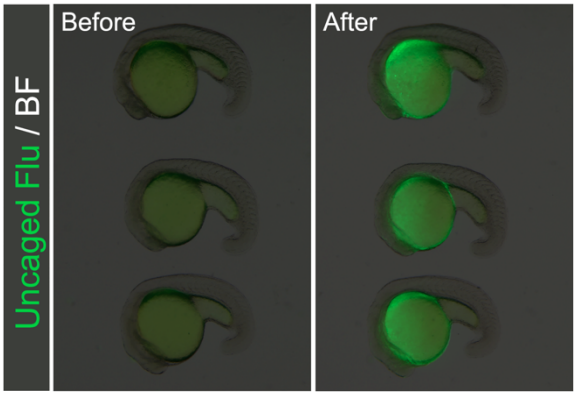

Fig. S6. *In vivo* rostral myeloid progenitors labeling with a photoactivatable cell tracer. At 20 hpf, after injection of caged fluorescein in the embryo at the 1-cell stage, the fluorescein in anterior part of embryo was uncaged with a pulsed ultraviolet [365 nm] laser beam.

Supplemental Figure 7

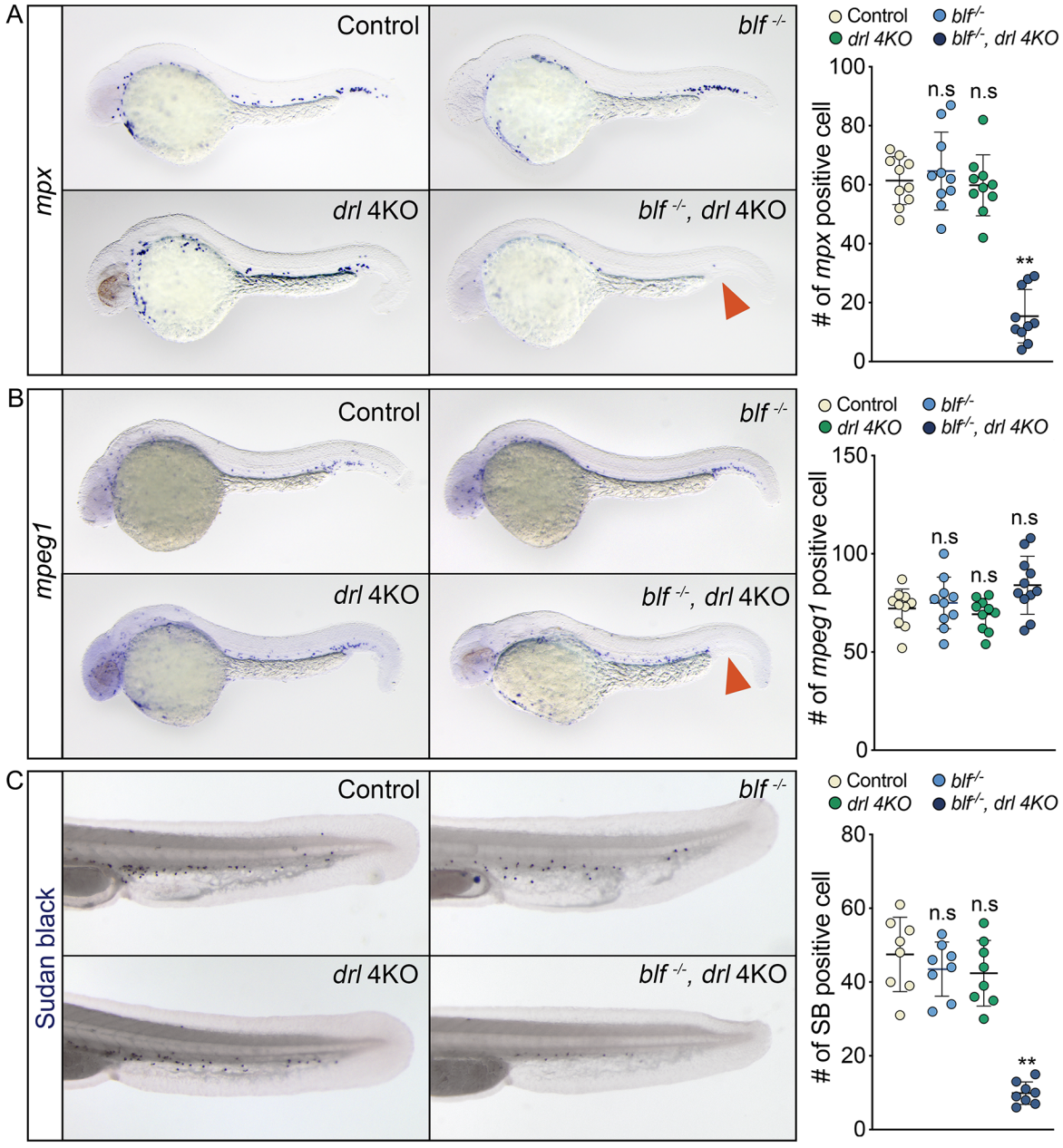

Fig. S7. The effect of loss of *blf* and *drl* cluster genes on intermediate myelopoiesis. (**A**) Left panels, RNA *in situ* hybridization results for expression of *mpx* in 36 hpf embryos. Right panel, scatter plot showing the mean number of *mpx*+ cells. (**B**) Left panels, RNA *in situ* hybridization results for expression of *mpeg1* in 36 hpf hpf embryos. Right panel, scatter plot showing the mean number of *mpeg1*+ cells. Red arrowheads in A and C indicates the lack of *in situ* hybridization

signal in posterior blood island (PBI). (**C**) Left panel, Sudan Black B (SB) staining of neutrophils in the CHT region in embryos at 36 hpf. Right panel, scatter plot showing the mean number of SB+ neutrophils. A, B and C, data are mean ± SEM, n.s, not significant, **P<0.01, ***P<0.001.

Supplemental Figure 8

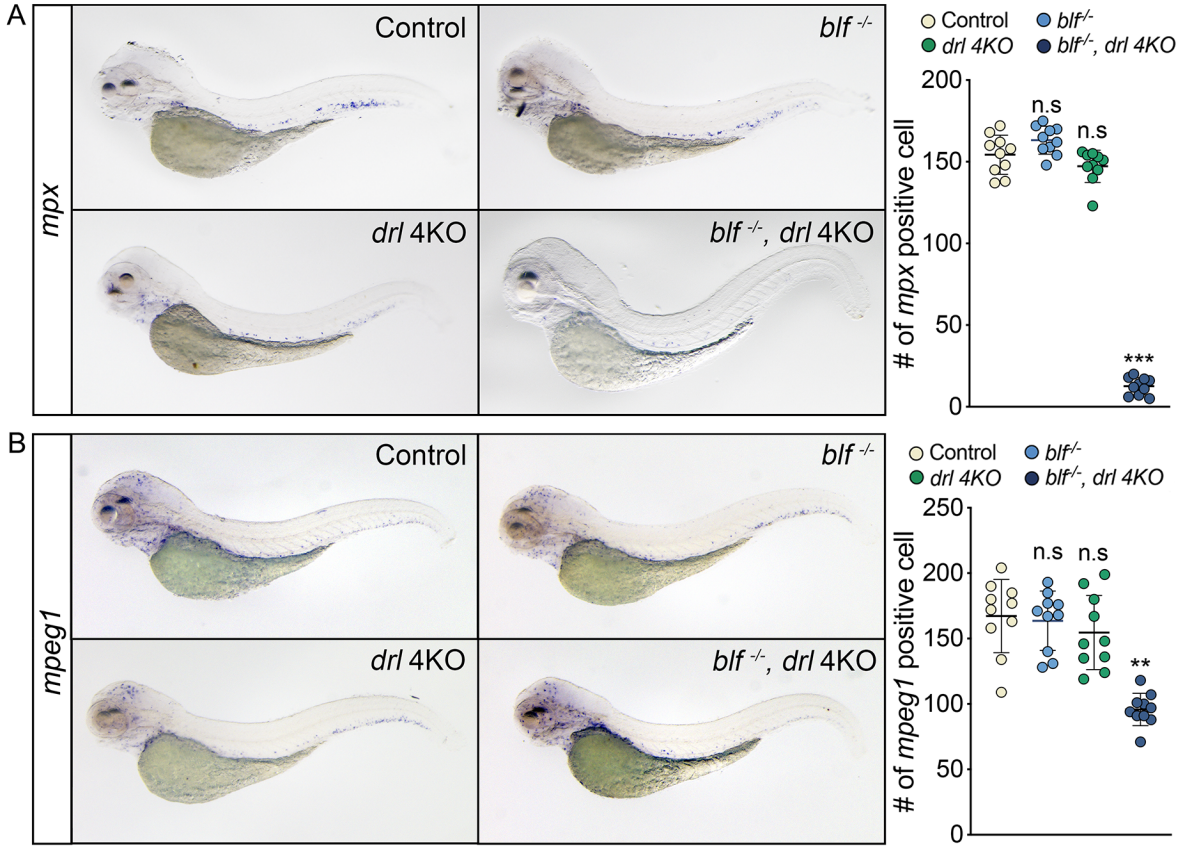

Fig. S8. The effect of loss of *blf* and *drl* cluster genes on definitive myelopoiesis. (**A**) Left panels, RNA *in situ* hybridization results for expression of *mpx* in 96 hpf embryos. Right panel, scatter plot showing the mean number of *mpx*+ cells. (**B**) Left panels, RNA *in situ* hybridization results for expression of *mpeg1* in 96 hpf embryos. Right panel, scatter plot showing the mean number of *mpeg1*+ cells. A and B, data are mean ± SEM. n.s, not significant. **P<0.001, ***P<0.0001.

Supplemental Figure 9

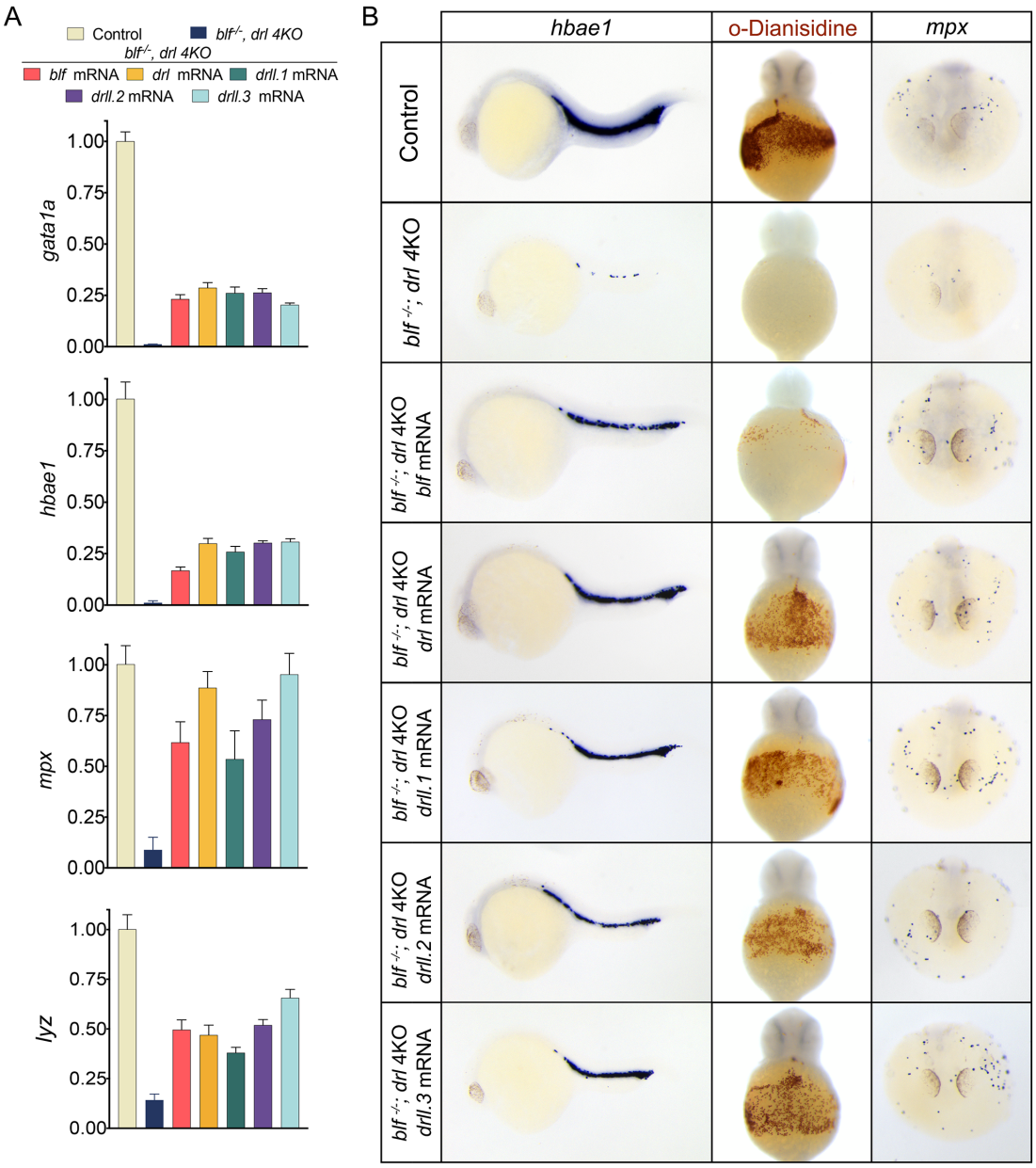

Fig. S9. *Blf* and *drl* cluster genes redundantly regulate zebrafish haematopoiesis. (**A**) QPCR results for expression of marker genes at 23 hpf in *blf*$^{-/-}$; *drl* 4KO embryos after mRNA injection. Data are mean ± SEM of at least three replicates. (**B**) Left panel, expression of *hbae1* in *blf*$^{-/-}$; *drl* 4KO embryos at 24 hpf embryos after mRNA injection, n=27, 39, 39, 36, 40, 30 or 38 for each experimental group. Lateral view with head to left. Middle panel, whole-mount O-dianisidine staining of 36 hpf embryos, ventral views, n=30, 37, 38, 31, 37, 31or 37 for each experimental

group. Right panel, RNA *in situ* hybridization results for expression of *mpx* in primitive neutrophils in 24 hpf embryos, frontal view, n=39, 32, 33, 33, 33, 39 or 33 for each experimental group.

Supplemental Figure 10

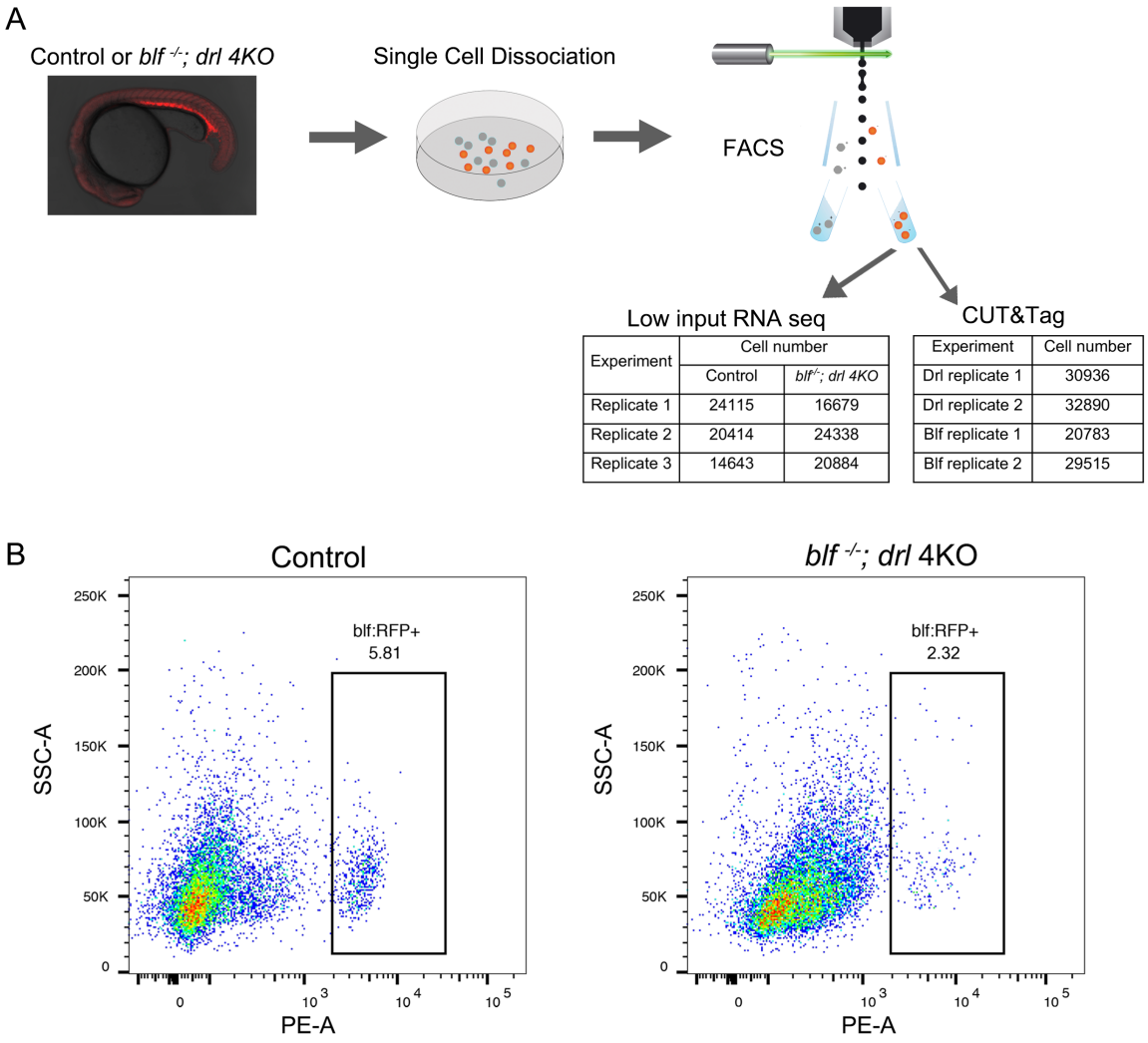

Experiment	Cell number	
	Control	*blf*$^{-/-}$; *drl* 4KO
Replicate 1	24115	16679
Replicate 2	20414	24338
Replicate 3	14643	20884

Experiment	Cell number
Drl replicate 1	30936
Drl replicate 2	32890
Blf replicate 1	20783
Blf replicate 2	29515

Fig. S10. Isolation and profiling of hematopoietic progenitors from control and *blf*$^{-/-}$; *drl* 4KO embryos. (**A**) Schematic of cell preparation. At 20 hpf, the whole embryo was dissociated into single cells, then RFP+ hematopoietic progenitors were isolated by FACS for downstream low input RNA sequencing or CUT&Tag sequencing. (B) Representative FACS plots of single cells with RFP fluorescence on the x-axis and side scatter area on the y-axis. RFP+ population (5.81% in control sample and 2.32% in *blf*$^{-/-}$; *drl* 4KO sample) displayed strong separation from the RFP- population.

Supplemental Figure 11

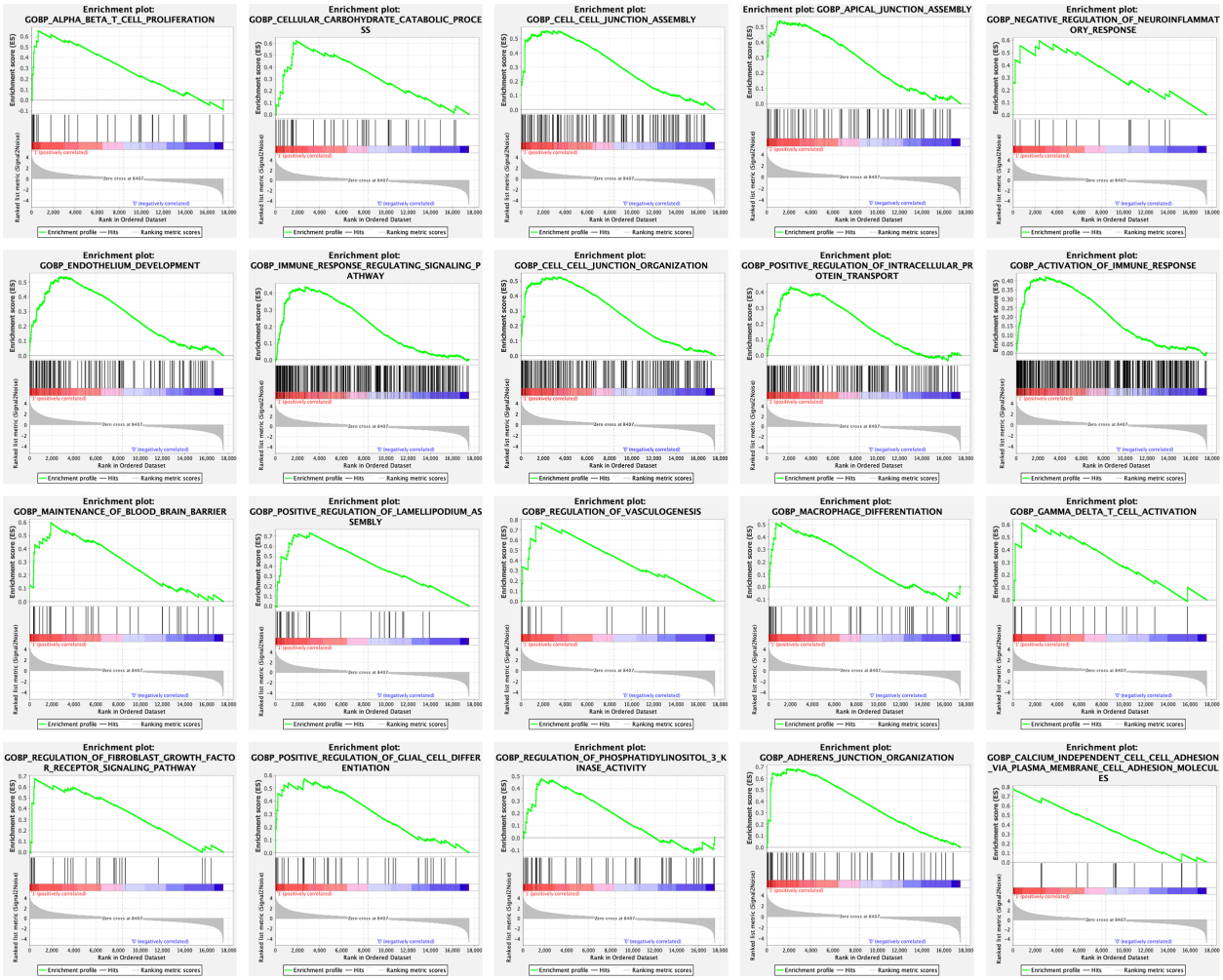

Fig. S11. GSEA analysis of the transcriptome dataset from control and *blf*$^{-/-}$; *drl* 4KO samples. Gene sets were ranked based on normalized enrichment score (NES) and top 20 sets were displayed.

Supplemental Figure 12

Transcription factor	Motif	p-value	% of targets	% of background
ZKSCAN1		1e-27	4.66%	1.40%
Gata3		1e-20	7.23%	1.78%
Stat3		1e-11	13.29%	4.91%
CEBP		1e-10	14.65%	11.65%
Gata1		1e-9	8.82%	2.90%
Klf1		1e-9	5.10%	3.38%
ZBTB33		1e-9	25.60%	9.59%
Nrf1		1e-9	11.16%	3.47%
Fosl2		1e-8	13.29%	5.38%
Klf4		1e-8	16.31%	4.11%

Fig. S12. Enriched sequence motifs identified by HOMER known motif analysis at Blf and Drl co-occupancy sites. The top 10 motifs are shown.

Supplemental Figure 13

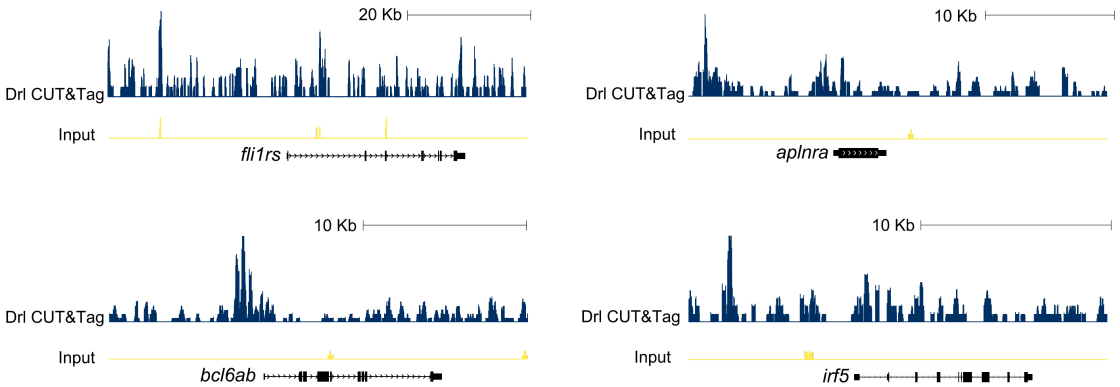

Fig. S13. Genome browser views of Drl binding profiles associated with *fli1rs*, *aplnra*, *bcl6ab* and *irf5*.

Supplemental Figure 14

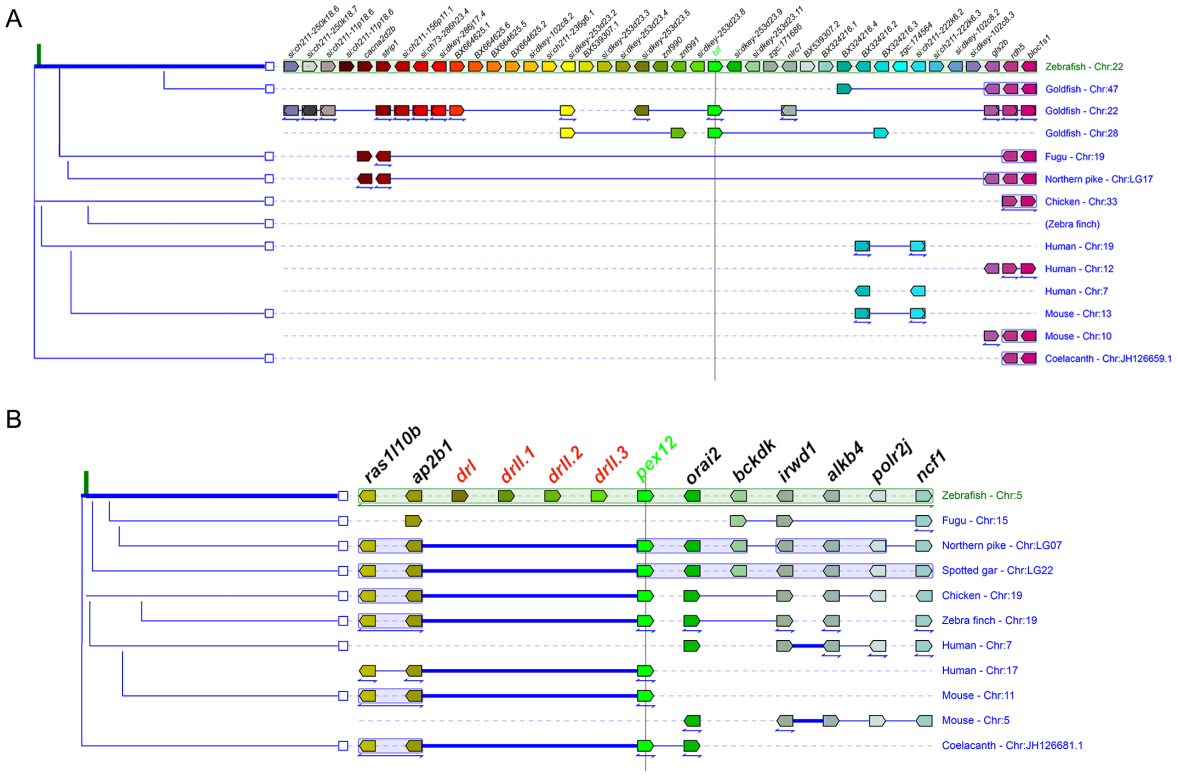

Fig. S14. Cross-species synteny analysis of *blf* and *drl* cluster. **A** and **B**, synteny diagram of the *blf* and *drl* cluster in zebrafish compare to other vertebrate animals.

Supplemental Figure 15

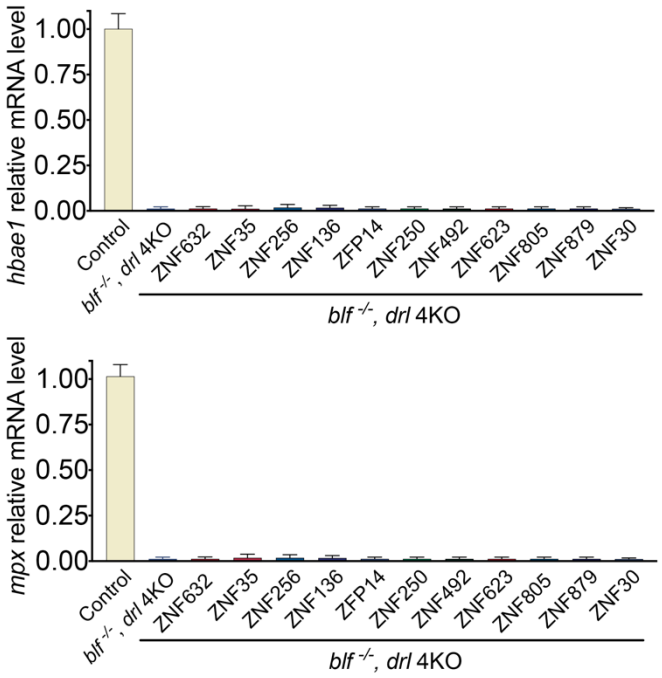

Fig. S15. Screening the mammalian functional ortholog of zebrafish *blf* and *drl* cluster genes. QPCR results for expression of erythroid mark genes *hbae1* and neutrophil marker gene *mpx* in ***blf*** $^{-/-}$; ***drl*** 4KO embryos after mRNA injection. Data are mean ± SEM of at least three replicates.

Supplemental Figure 16

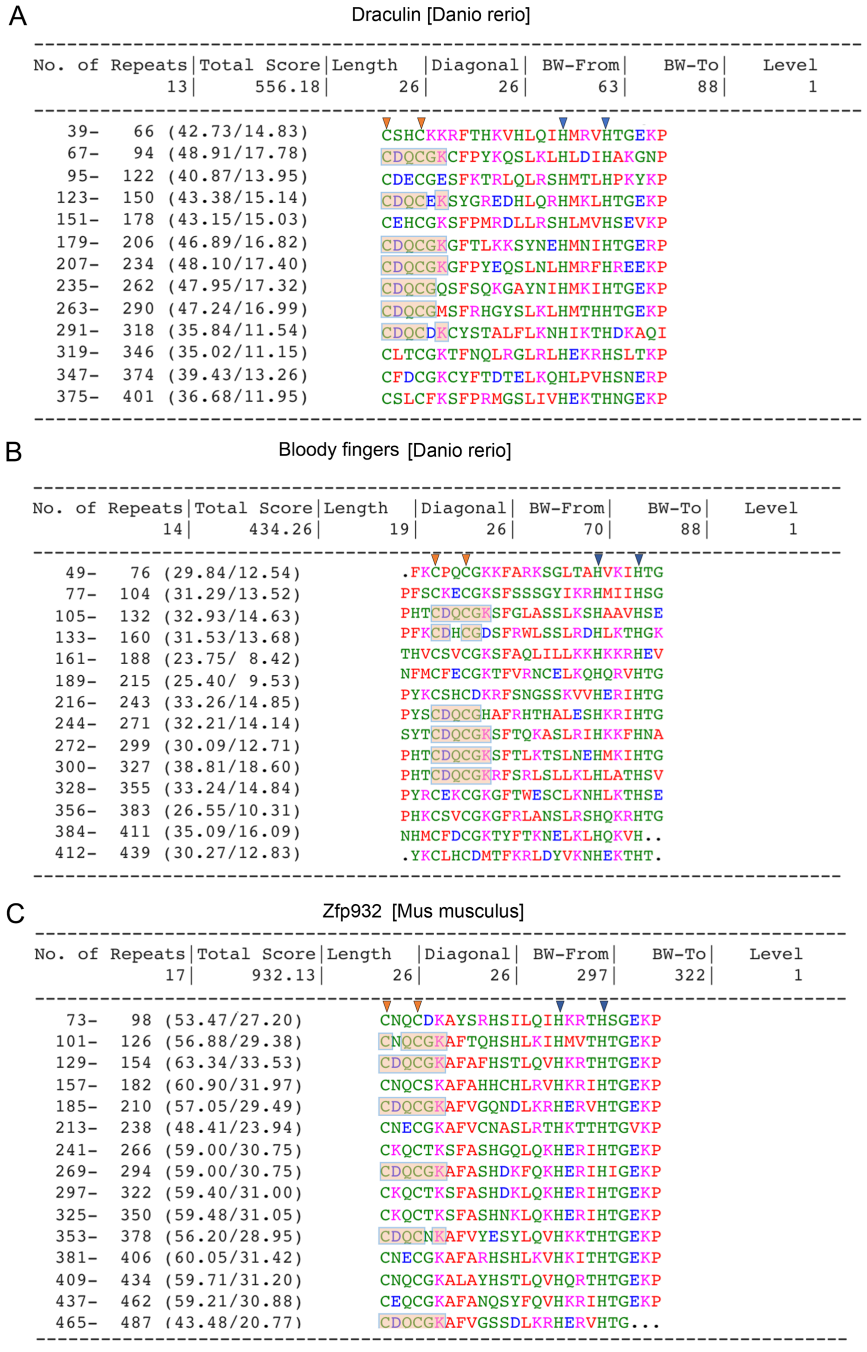

Fig. S16. Repeated sequence motifs of Drl, Blf and Zfp932 identified by RADAR. BW, best window. Orange and blue arrowheads indicate the cysteine and histidine residues on C2H2 Zinc finger.

Table S1. Differential expression genes between *blf* $^{-/-}$,drl 4KO and control cells.

Click here to download Table S1

Table S2. List of Drl and Blf binding regions in blf:RFP+ cells.

Click here to download Table S2

Table S3. List of direct downstream genes of Drl.

Click here to download Table S3

Table S4. Mammalian ortholog candidates of zebrafish *blf* and *drl* cluster genes

Name	NCBI Ref. Seq	E-value	Secondary Structure Scores	Aligned cols	Target Length
ZNF266	NP_006622.2	1.70E-49	36.6	398	549
ZNF101	NP_001287878.1	1.00E-48	35.4	316	316
ZNF632	XP_047297102.1	1.80E-49	34.8	409	543
ZNF226	NP_001027545.1	1.00E-48	34.8	408	803
ZFP932	NP_663538.2	1.60E-49	34.6	411	526
ZNF35	NP_003411.3	1.00E-48	34.4	406	527
ZNF256	NP_001362332.1	2.10E-49	34.2	396	474
ZNF136	NP_001334943.1	4.50E-49	34.2	369	508
ZFP2	NP_085116.2	3.40E-49	34.1	410	461
ZFP14	NP_001284548.1	5.40E-49	34.1	394	534
ZNF184	NP_001305820.1	5.70E-49	34.1	409	751
ZNF180	NP_001265438.2	1.00E-48	34	409	665
ZFP345	NP_001030072.2	1.30E-49	33.9	398	561
ZFP950	NP_001296145.1	8.20E-49	33.8	408	609
ZFP184	NP_898835.1	1.30E-49	33.3	406	737
ZNF345	NP_001229401.1	3.00E-49	33	403	488
ZNF595	NP_872330.1	7.60E-49	32.5	391	648
ZNF250	NP_001103159.1	6.10E-49	31.2	394	555
ZNF492	NP_065906.1	9.90E-49	29.9	401	531
ZNF623	NP_001075949.1	5.40E-49	29.4	405	496
ZNF805	NP_001138550.1	6.10E-49	29	411	494
ZNF879	NP_001129588.1	1.30E-49	28.6	392	563
ZNF30	NP_001307595.1	1.30E-49	28.4	395	519
ZNF429	NP_001333842.1	1.00E-48	26.7	395	642

Candidates were ranked according to secondary structure scores . Aligned Cols', lengths of the aligned region. Target Length, lengths of the candidate protein.

Table S5. Primers for quantitative real-time RT-PCR analysis.

Click here to download Table S5